

Accelerance Decoupling: An Approach for Removing the Influence of the Test Stand from the Integrated Modal Test

Joel W. Sills Jr.

NASA Johnson Space Center
2101 NASA Parkway
Houston, TX 77058

Daniel Kaufman

NASA Goddard Space Flight Center
8000 Greenbelt Road
Greenbelt, MD 20771

Arya Majed

Applied Structural Dynamics
Houston, TX 77024

ABSTRACT

The main objective for launch vehicle (LV) modal testing is to quantify the LV's modal properties in the free-free state (post pad separation). However, given the size of most LV systems, free-free testing is a challenge and often not feasible. With this, a test stand, typically the launch pad itself, is introduced as the means of support. This shifts the challenge to developing robust numerical methods for removing the influence of the launch pad from the integrated system modal test. The Space Launch System (SLS) is no exception where the mobile launcher (ML) is used to support the vehicle for the integrated modal test (IMT). For the IMT, it is well understood from pre-test analysis with finite element models (FEMs) of the SLS and SLS coupled to ML that the ML has a significant influence on the SLS modal properties especially in the lower frequency range where the primary SLS bending modes exist. An accelerance decoupling (AD) method has been formulated for the purpose of "subtracting out" the influence of the ML from the IMT results. With AD, the SLS decoupled frequency response functions (FRFs) are directly extracted from the IMT FRFs. The subject approach is aimed to utilize measured data only and achieve a robust FRF decoupling scheme. AD is derived from a widely used coupling technique called "Receptance Coupling" (RC). The AD core equation reverses the RC process and utilizes a pair of auxiliary equations that enable the core equation to be resolved based on measured data only. In AD, the decoupled component FRFs are extracted from the coupled system FRFs with a transformation to remove the contribution of the "subtractive component". This paper addresses the AD's operational flexibility to resolve SLS free-free modal properties from coupled system measured data but also the possibility to include data from FEM if there is enough confidence in the FEM or if it is asserted that the effect to the final outcome is reasonable.

Keywords: Accelerance Decoupling, Receptance Coupling, Frequency Response Function, Finite Element Model

ACRONYMS

AD	Accelerance Decoupling
CLA	Coupled Loads Analysis
CS	Core Stage
DMM	Dynamic Math Model
DoF	Degrees of Freedom
ESD	Exploration Systems Development

FEM	Finite Element Model
FRF	Frequency Response Function
FWD	Forward
HDP	Hold Down Point (booster aft skirt)
Hz	Hertz
IFF	Interface Force
IMT	Integrated Modal Test
IOP	Ignition Over Pressure
L&D	Loads and Dynamics
lbs	Pounds
LSRB	Left Side Booster
LV	Launch Vehicle
ML	Mobile Launcher
MSO	Mass Simulator for Orion
RC	Receptance Coupling
Rms	Root-Mean-Squared
RFMB	Residual Flexibility Mixed Boundary
RSRB	Right Side Booster
SLS	Space Launch System
SRB	Solid Rocket Booster
VSP	Vehicle Support Post
VSS	Vehicle Stabilization System

INTRODUCTION

The SLS family of vehicles will be stacked, rolled out, and launched from the ML. The ML consists of an Ares I derived tower structure and a Space Shuttle derived base structure. The ML tower will supply power, propellant, personnel access, and lateral support to the vehicle. The ML base is the platform on which the vehicle is vertically supported during its assembly, rollout, and prelaunch. There are eight vehicle support posts (VSPs) on the ML base that constrain the vehicle to the pad; four VSPs constrain the aft skirt of the left-hand booster and four VSPs constrain the aft skirt of the right-hand booster. Figure 1 provides an integrated model of the SLS stacked system with the Mass Simulator for Orion (MSO) sitting atop the ML. This configuration serves as the Integrated Modal Test IMT.

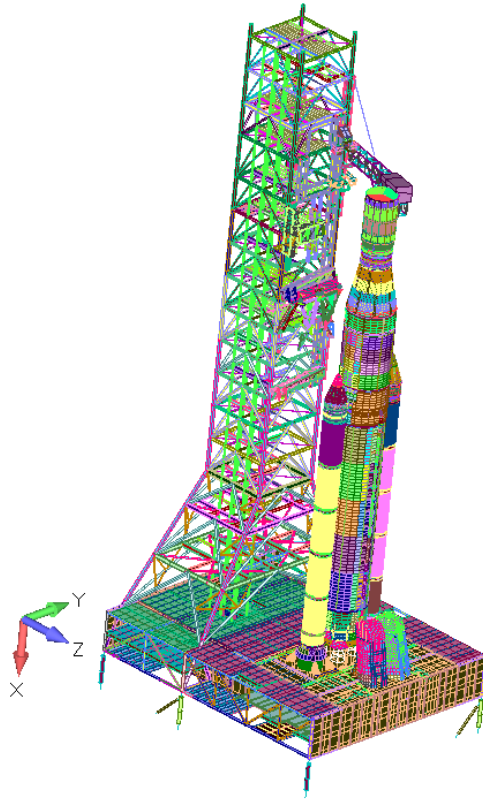


Figure 1. Finite Element Model Representation of the Integrated Stacked SLS System with the MSO on the ML

The primary IMT challenge is discerning the coupling of the SLS vehicle stack with the ML. The SLS is flight hardware and as such there are detailed drawings, traceable plans, and well-developed models. The ML is a large steel structure and has many modes in the frequency range of interest for the SLS and so its influence cannot be neglected. Decoupling of the SLS vehicle stack from the complete “test article” should rely on a low-risk strategy. To address this challenge, the ML underwent a modal to characterize its dynamic properties and model updates were made. To date, all that is available are FEM simulations using uncorrelated models.

Given the complexity of using a flexible structure as a test fixture, a solicitation call went out to the NASA community for decoupling methods. As a response, both fixed base and free-free modal parameter extraction methods were proposed. The fixed base methods included a method developed by Napolitano [1, 2] and the dynamic substructuring method developed by Allen and Mayes [3]. The subject method, AD, was presented as a free-free decoupling method.

The problem that AD attempts to address is: Given SLS + ML and ML stand-alone acceleration (FRF of acceleration normalized to force), find the SLS free-free acceleration. Figure 2 depicts this problem in a simplified graphic. Determining the ML stand-alone acceleration is required to remove its influence from the coupled system.

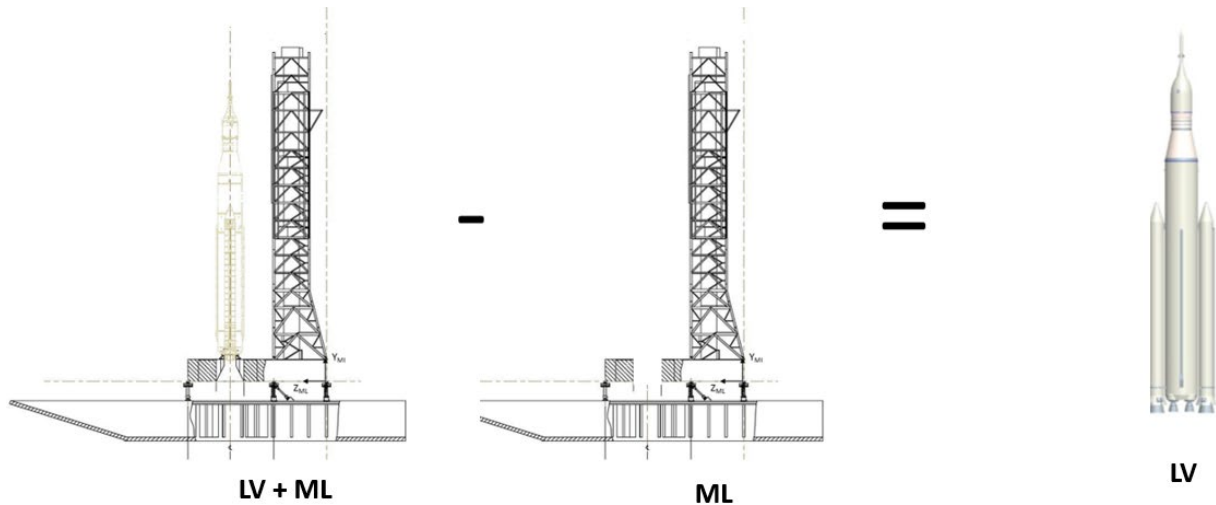


Figure 2. Conceptual Accelerance Decoupling; (Launch Vehicle (LV) = SLS)

METHODOLOGY

The AD “core” equation is derived from a series of simple ‘thought experiments’ and algebraic manipulations which reverse the Receptance Coupling (RC) process. Prior to this development, extensive work using RC coupled with Norton-Thevenin (NT) produced a Norton Thevenin Receptance Coupling (NTRC) methodology [16 (also see 4 and 5 for background)] for fast coupled loads analysis.

Figure 3 describes the notation system utilized for AD. In this figure, **a** denotes the SLS, **b** the ML, and **c** the coupled SLS + ML system. DoF sets are defined as:

- s**: connecting DoFs between SLS and ML
- r**: SLS response measurement DoFs
- f**: force application DoFs (subset of r)
- t**: ML DoFs

In addition, **A** denotes the acceleration vector, and **H** the accelerance matrix.

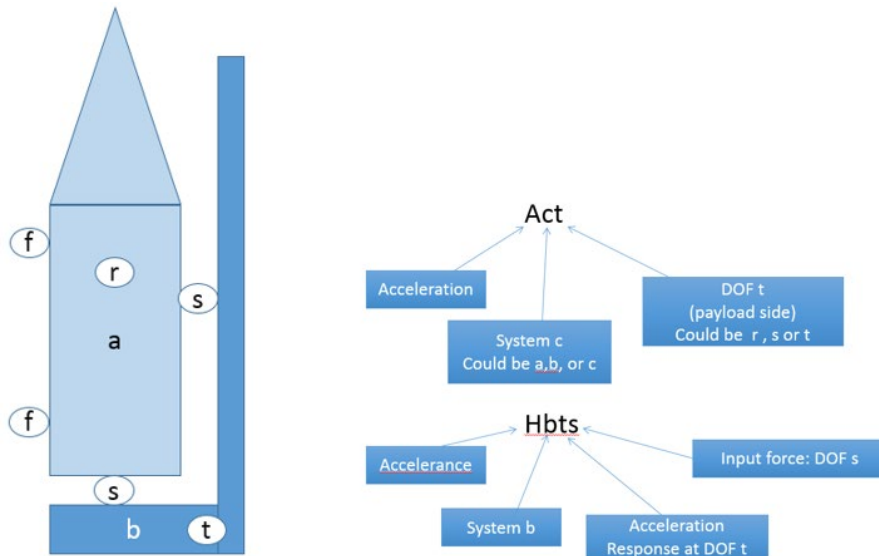


Figure 3. AD Notation System

Using this formulation, one can develop a relationship for the IMT configuration. From Reference 4, the system accelerance matrix can be written using receptance coupling for the SLS (System a) and the ML (System b) as shown in equation (1).

From Reference 4, the system accelerance matrix can be written using receptance coupling equation (1):

$$\begin{bmatrix} H_{crr} & H_{crs} & H_{crt} \\ H_{csr} & H_{css} & H_{cst} \\ H_{ctr} & H_{cts} & H_{ctt} \end{bmatrix} = \begin{bmatrix} H_{arr} & H_{ars} & 0 \\ H_{asr} & H_{ass} & 0 \\ 0 & 0 & H_{btt} \end{bmatrix} - \begin{bmatrix} H_{ars} \\ H_{ass} \\ -H_{bts} \end{bmatrix} [H_{ass} + H_{bss}]^{-1} \begin{bmatrix} H_{ars} \\ H_{ass} \\ -H_{bts} \end{bmatrix}^T \quad (1)$$

The fundamental thought experiment in AD is to reverse this coupling process into a decoupling process. This is done through a simple algebra exercise on equation (1) to solve for H_{arr} or more precisely, a column partition of H_{arr} , H_{arf} – the decoupled accelerance of the SLS (e.g., accelerometer rows, excitation columns). H_{arf} is the quantity to be solved for and can be expressed as equation (2):

$$H_{arf} = H_{crf} + H_{ars}(H_{ass} + H_{bss})^{-1}H_{asf} \quad (2)$$

Equation (2) is the AD core equation that provides the desired SLS free accelerance as a function of the coupled SLS + ML accelerance. However, the equation does include component **a** data blocks, which must be expressed in terms of the coupled system **c** for this to be a fully test driven methodology. This is accomplished through further algebraic manipulations of equation (1) resulting in the set of auxiliary equations (3) and (4):

$$H_{ars} = H_{crs}[I_{ss} - (H_{ass} + H_{bss})^{-1}H_{ass}]^{-1}, \quad (3)$$

$$H_{asf} = [I_{ss} - H_{ass}(H_{ass} + H_{bss})^{-1}]^{-1}H_{csf}, \quad (4)$$

and an auxiliary equation (5) from the flexibility relationship at the component interfaces:

$$H_{ass} = H_{css} - H_{css}(H_{css} - H_{bss})^{-1}H_{css}. \quad (5)$$

Equations (3), (4), and (5) demonstrate the calculation of H_{arf} requires accelerance data blocks: H_{crf} , H_{crs} , H_{csf} , H_{css} , and H_{bss} . The first four data blocks are from the coupled SLS + ML system, and the final data block is from the stand-alone ML test. Note a reduced version of this formulation was also developed by the team which utilizes the same five key data blocks in a more direct manner. However, this reduced formulation has not been verified. Note from the above formulation, AD can be utilized directly with test-derived data or in a “hybrid” mode utilizing a combination of test and model derived data.

Some further background material that may prove useful as a primer includes: Reference 6 which provides a comparison of FRF and modal methods for combining experimental and analytical substructure; reference 7 which provides a method for improving experimental frequency response matrices for admittance modeling; reference 5 which discusses the FRF Based Substructuring and Modal Synthesis; reference 8 which provides a general framework for dynamic substructuring and classifies the different types of methods; reference 9 which provides a treatment for uncertainty propagation in experimental dynamic substructuring; reference 10 which discusses modal testing of “delicate and critical” structures; Reference 11 which discusses “lightly damped experimental substructures for combining with analytical substructures.”; reference 12 which discusses removing undesired periodic data from random vibration data; reference 13 which provides a method for using modal test data to estimate support properties; and finally, reference 14 which provides a method for substructure identification from coupled system test data.

MODELS

The AD verification involves models in a similar configuration to the IMT: (1) SLS prelaunch integrated system model, and (2) the ML. The SLS is an over-constrained Hurty Craig-Bampton dynamic math model (DMM) with 3992 DoFs. Retained nodes include the centerlines, actuators/gimbals, and others. The ML is a residual flexibility mixed-boundary (RFMB) [15] DMM. Retained DoFs include posts to ground, vehicle support posts (VSPs), and Vehicle Stabilizer System (VSS). The SLS prelaunch CLA DMM is shown in Figure 4 and the ML FEM is shown in Figure 5. For this exercise, the Vehicle Stabilizer System (VSS) is included as it provides a structural interface to the SLS for rollout and liftoff. During the IMT, the VSS will not be connected and the SLS will be solely supported by the VSPs.

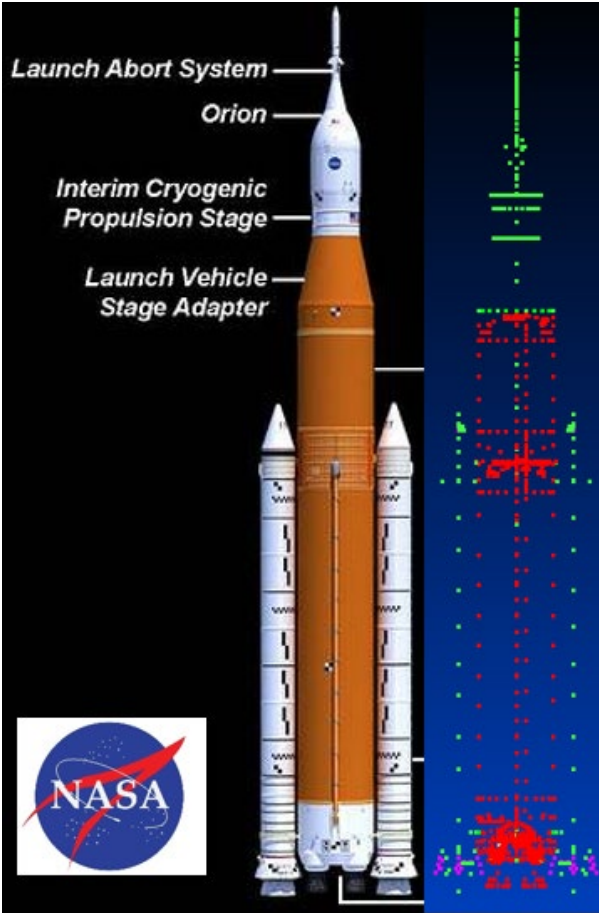


Figure 4. SLS DMM Retained Nodes



Figure 5. ML FEM Utilized in this Study

Gravity (i.e., application of 1G) quasi-static input model checks were performed to verify proper analytical integration. The right and left boosters (RSRB and LSRB), VSP and the VSS interface forces were computed on the ML side of the interface. Note that no stacking preload logic [16] was utilized for this 1G checkout.

RECEPTANCE COUPLING - CHECKOUTS

The first step after completing model checks applied Equation 1, the fundamental RC relationship and compare results to outputs from a traditional coupled loads analysis (CLA). This step verifies the accuracy of the data-blocks that will be utilized in the AD calculations. A set of input forcing function with a constant amplitude equal to 100 lbs. in X, Y, and Z SLS over a frequency range of 0.1 to 50 Hz drove the coupled system at the forward (FWD) solid rocket booster (SRB) attach location. Modal damping of 1% was applied to all free-free modes. A sample SLS internal acceleration item (e.g., core stage (CS) engine section boattail ignition over pressure (IOP) grid) is shown in Figure 6.

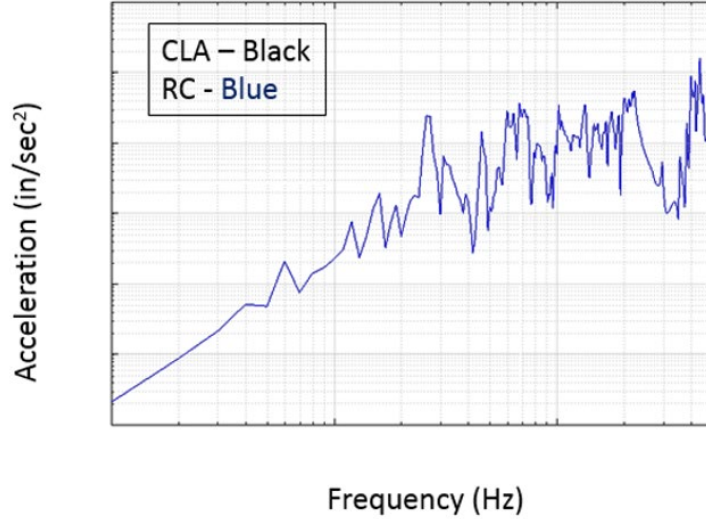


Figure 6. Comparison of Receptance Coupling (RC) (Equation 1) to CLA

Overall, 30 interface forces, 30 interface accelerations, and 24 internal acceleration were recovered and compared. All comparisons were within numerical noise thresholds. This verified the data blocks for subsequent AD usage were accurately calculated.

SLS COUPLED VERSUS FREE RESPONSE

A CLA was performed next to compute the SLS free response, which will serve as the benchmark for AD comparisons. With the SLS + ML (i.e., coupled) response from the receptance coupling checks, the two spectra can be compared for various response items. Figure 7 shows this comparison for a booster/ML VSP tie-down. It is seen the acceleration for the free-free SLS at the low frequency are dominated by the “mass line,” which is a function of the SLS rigid-body mass and moment of inertia properties. The accelerations for the coupled SLS + ML system are dominated by the “stiffness line” at the low frequencies, which is a function of the SLS/ML interface flexibilities.

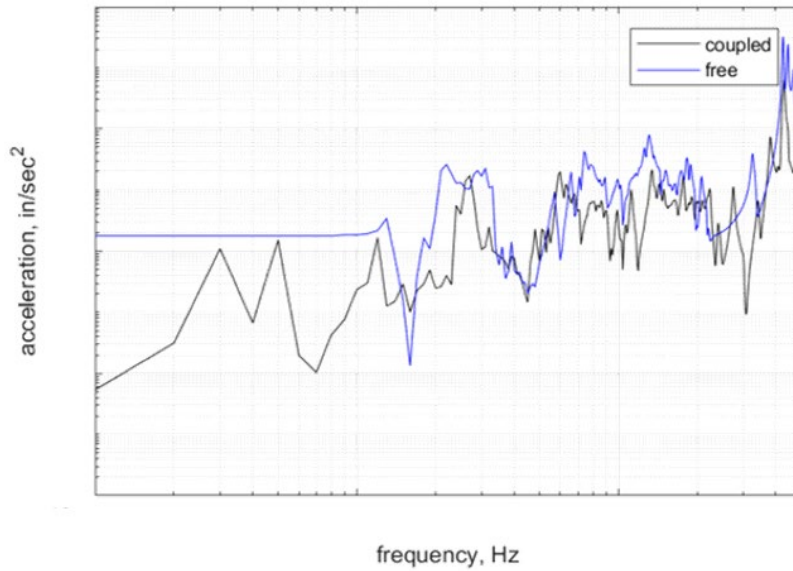


Figure 7. Comparison of SLS Coupled and Free Response (VSP)

It is observed that the SLS when free versus coupled to the ML display measurable differences in acceleration response. Note that AD must start with coupled system data and must overcome this difference to be a viable method.

ACCELERANCE DECOUPLING VERIFICATION AND STRESS TESTING

The AD methodology was used to extract the SLS free response from the SLS + ML coupled system response. A sample SLS internal acceleration item (e.g., CS engine section boattail IOP grid) is shown in Figure 8.

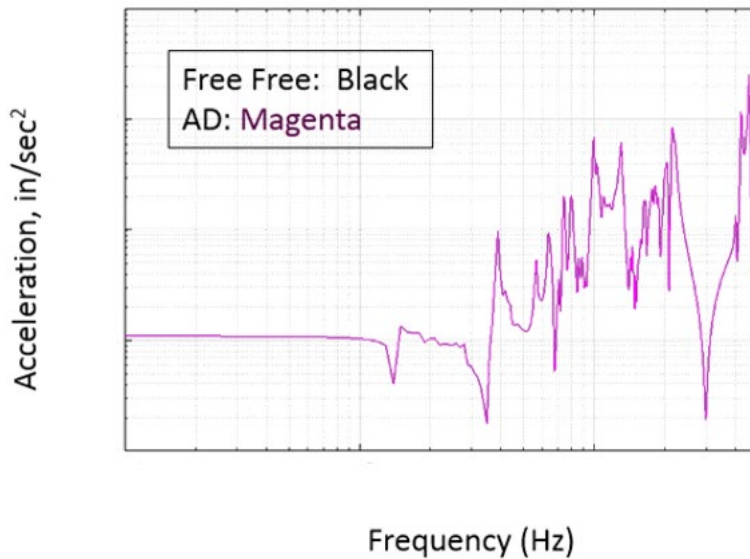


Figure 8. Comparison of Free-Free SLS Response (Exact) to Response Extracted from Coupled System using AD

Again, 30 interface forces, 30 interface accelerations, and 24 internal accelerations were recovered and compared. All comparisons were within numerical thresholds. This verified that the AD methodology can extract the SLS free-free response from SLS + ML coupled system response.

The results to this point demonstrate that the methodology can decouple the SLS free-free responses from the coupled system. However, the method needs to demonstrate robustness in the presence of the following: ML VSP to Booster rotational DoFs stiction; ML acceleration perturbations; and in the presence of instrumentation noise.

All AD simulations modeled the ML to booster interface as a ball jointed interface. The IMT will introduce multi-point excitation at low frequency and varying amplitudes into the coupled SLS + ML system. It is entirely likely the ball-jointed ML to booster interfaces may be rotationally constrained when subjected to this low-level input. As such, an effort was made to model the subject interface inclusive of rotational DoFs stiction (via rotational constraints). This doubles the size of the interface acceleration matrices and introduces local moments into the problem. If numerical issues due to acceleration inversions were to be introduced, it would be detected here as a bad comparison back to the benchmark free SLS results. Figure 9 provide an example comparison of SLS free response (i.e., benchmark) to that calculated using the AD procedure. It is seen this procedure accurately dissects the SLS free acceleration response from the coupled SLS + ML response resulting in a near perfect match.

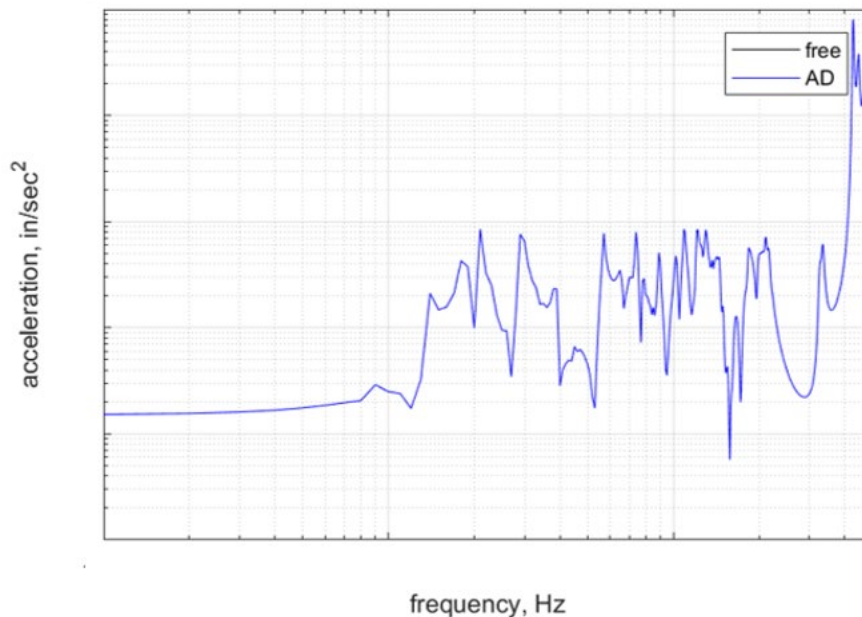


Figure 9. Booster Aft Skirt Acceleration

Variants of the stiction investigations assume that the coupled system still includes rotational DoFs stiction while, the subtractive component, the ML, will not be able to react the local moments. This inconsistency in boundary conditions between the coupled system and the subtractive component produces some level of error in the AD calculation. The implementation for this stress test includes coupled system rotational stiction at all eight VSP ball joints; ML (subtractive component) with only translational acceleration available at VSP ball joints; and the AD method: $SLS = \text{Coupled System} - ML$. With ML VSP rotational acceleration data not available, the ML acceleration is no longer consistent with coupled system stiction state. This will result in an error in AD attempt to decouple the vehicle from coupled system acceleration. Two subcases were evaluated including: Case 1: ML rotational acceleration available at all VSPs except VSP-1 and Case 2: ML rotational acceleration not available at any VSPs. Case 1 is a numerical sanity check or checkout and Case 2 is a stress test. Figure 10 provides a graphical layout of the VSP interfaces along with their numbering.

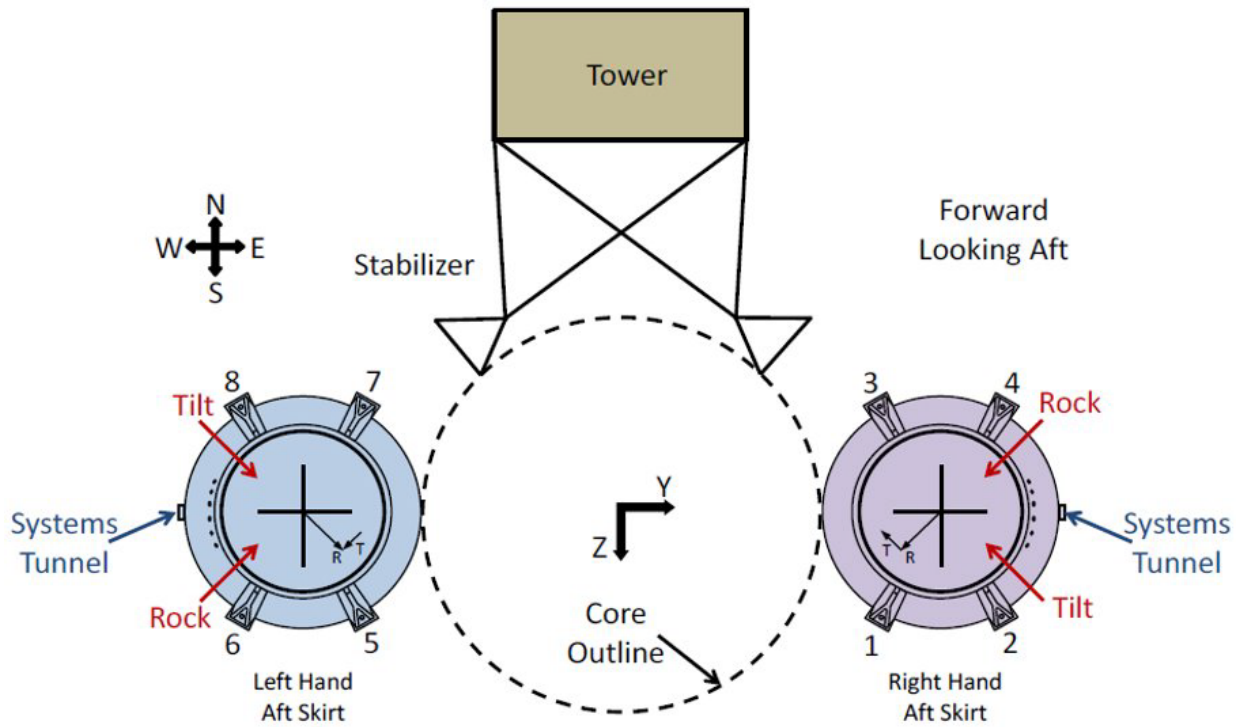


Figure 10. ML VSP Layout Numbering

Figures 11 and 12 provide the AD results for the booster aft skirt accelerations – VSP1 X and booster aft skirt accelerations – VSP1 Y respectively. Case 1 (checkout) shows minor impact at VSP1 only with other VSPs mostly unaffected and matches expectations.

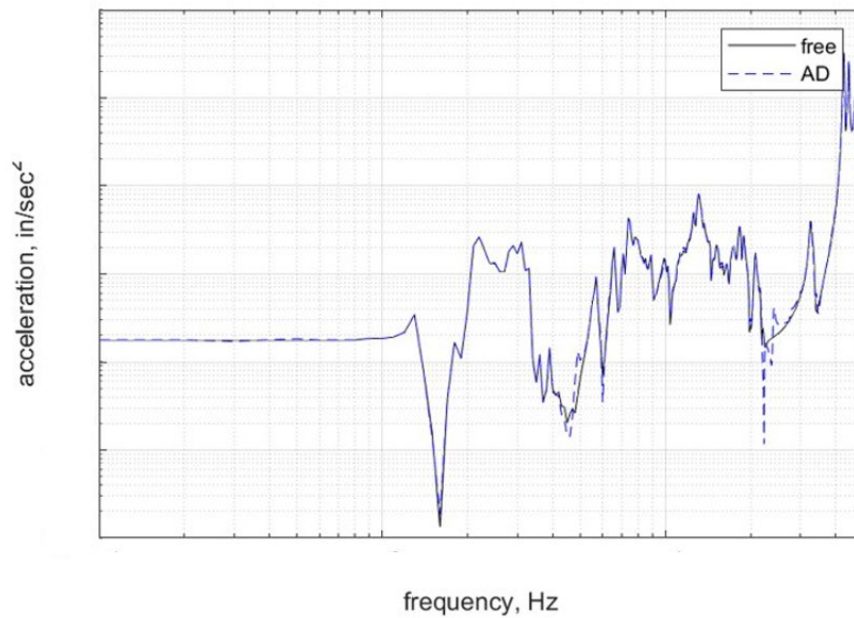


Figure 11 Booster Aft Skirt Accelerations – VSP1 X

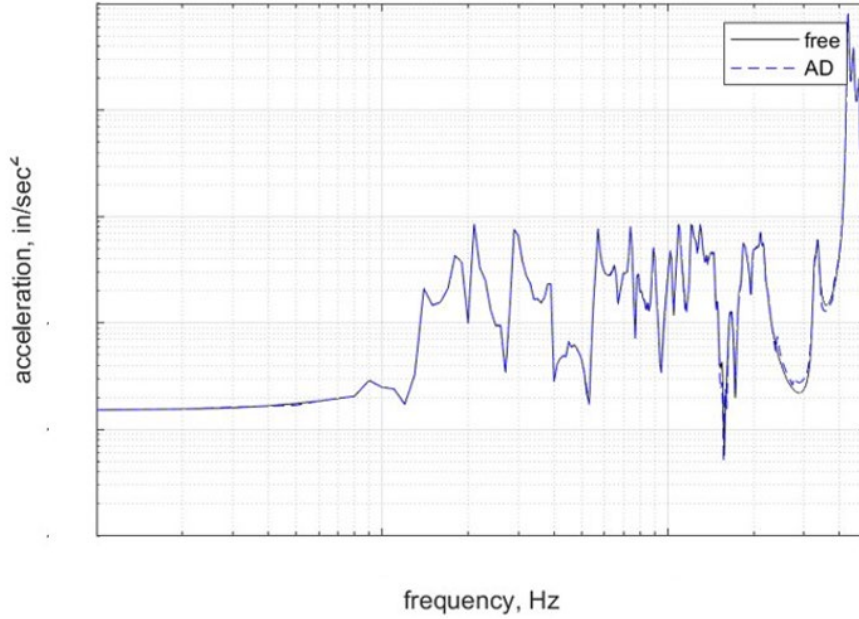


Figure 12. Booster Aft Skirt Accelerations – VSP1 Y

Figures 13 and 14 show the AD results for the booster aft skirt accelerations; VSP1 X and booster aft skirt accelerations; and VSP1 Y respectively. Case 2 (i.e., stress test) shows minor impact at all VSP locations. From this exercise, AD remained computationally robust under VSP stiction. There was some impact, which seems to be constrained mostly to the “valleys” of the FRFs. This should mitigate curve fitting concerns.

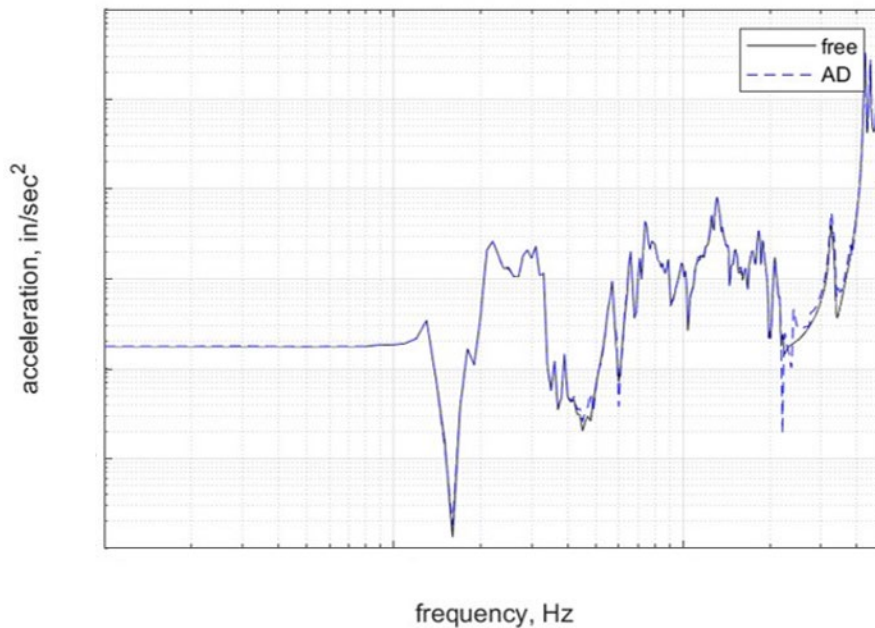


Figure 13. Booster Aft Skirt Accelerations – VSP1 X

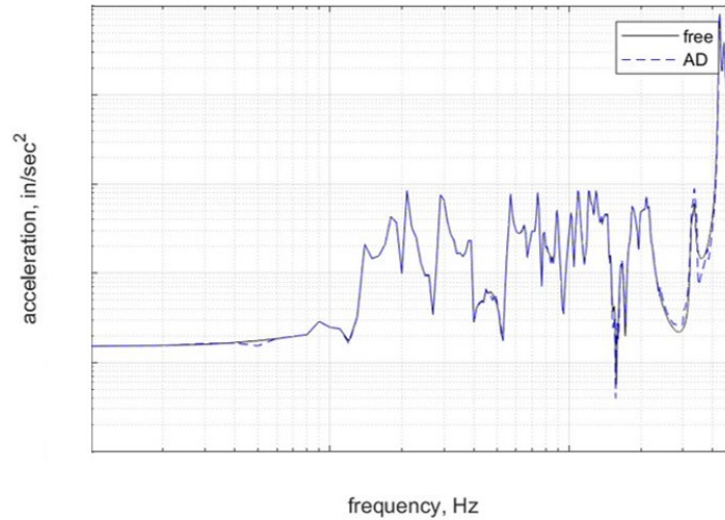


Figure 14. Booster Aft Skirt Accelerations – VSP1 Y

ML damping variations were introduced to study acceleration perturbation effects. This study assessed AD computational sensitivity to perturbations of ML acceleration (e.g., subtractive component) while keeping the coupled SLS + ML acceleration unchanged. Initially, eleven separate AD constructions were performed to address an $\pm 5\%$ perturbation of nominal damping in 1% increments. Additional runs to evaluate $\pm 10\%$ perturbations of nominal damping were performed as well. The rationale behind this exercise is that the ML being both a jointed and welded structure may have values ranging from lightly damped (i.e., 0.5 to 1%) to higher damped (i.e., 3 to 5%). Figures 15 and 16 provide a comparison of SLS nominal free response (i.e., benchmark) to that calculated using the AD procedure inclusive of ML acceleration damping perturbations. In all, the AD process remains computationally robust under ML acceleration perturbations. There was some impact that seem to be constrained mostly to the FRF “valleys,” which should minimize curve fitting concerns.

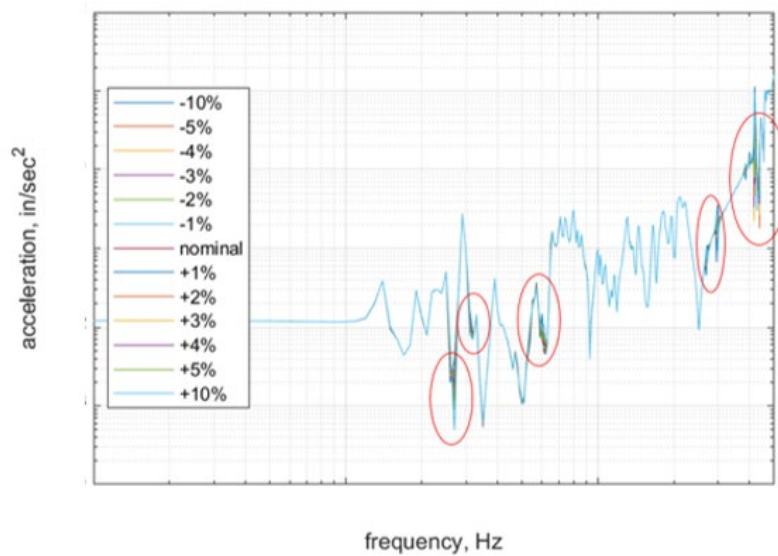


Figure 15. Booster Aft Skirt VSP1 Acceleration X

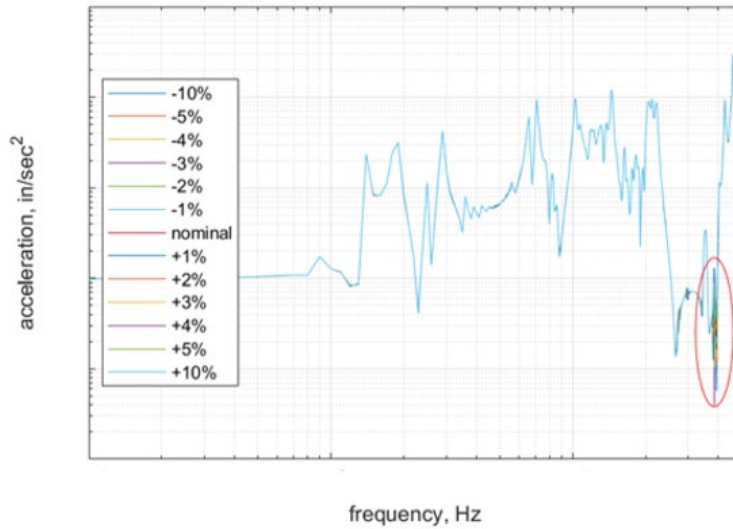


Figure 16. CS Engine Section Node

The AD formulation underwent further stress testing by perturbing the subtractive component by varying the component frequency. In this case, the coupled system remains unchanged. This inconsistency in modal properties between the coupled system and subtractive component will produce some level of error in the AD procedure. For this case, the ML (i.e., subtractive component) has its component frequencies varied by $\pm 5\%$. Ultimately, this exercise seeks to understand with the ML acceleration data no longer consistent with coupled system how much error will be incurred when the AD process attempts to decouple the vehicle from coupled system acceleration. Figures 17 and 18 show the AD results for ML at 1.05 x nominal frequencies at the booster aft skirt accelerations – VSP1 X and booster aft skirt accelerations – VSP1 Y respectively.

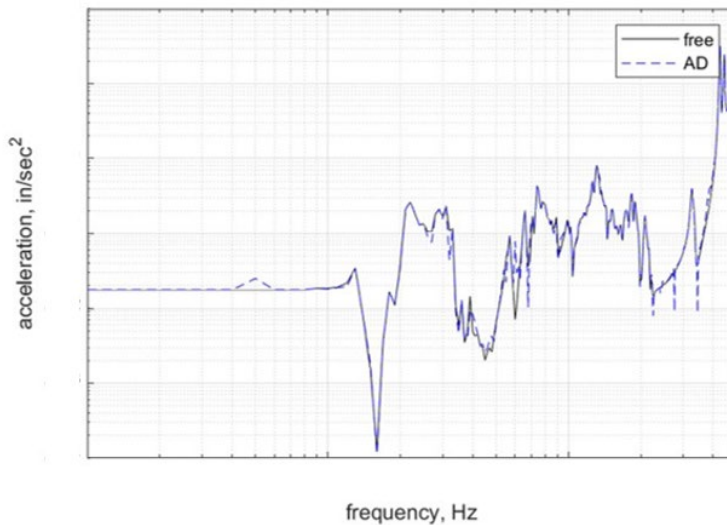


Figure 17. Booster Aft Skirt VSP1 Acceleration X

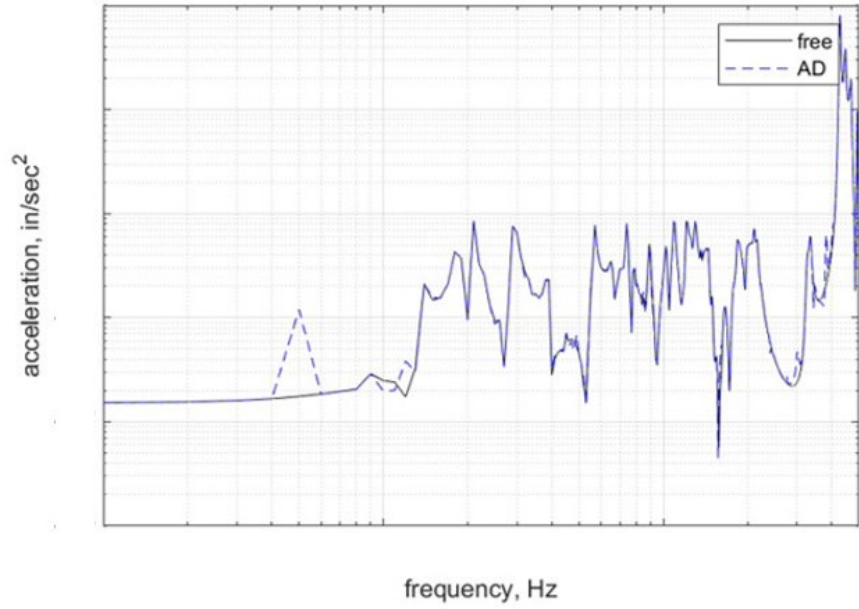


Figure 18. Booster Aft Skirt VSP1 Acceleration Y

Figures 19 and 20 show the AD results for ML at 0.95 x nominal Frequencies at the booster aft skirt accelerations – VSP1 X and booster aft skirt accelerations – VSP1 Y respectively.

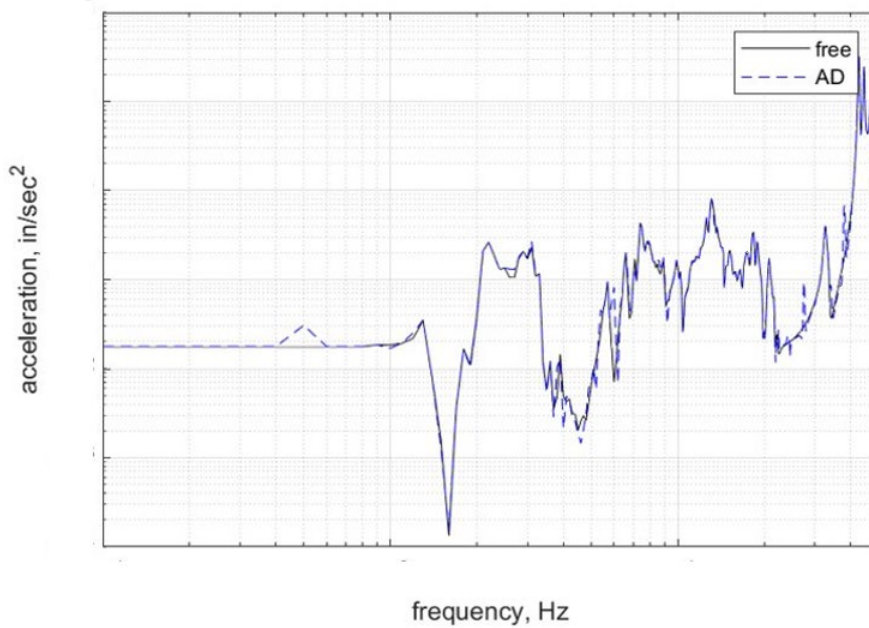


Figure 19. Booster Aft Skirt VSP1 Acceleration X

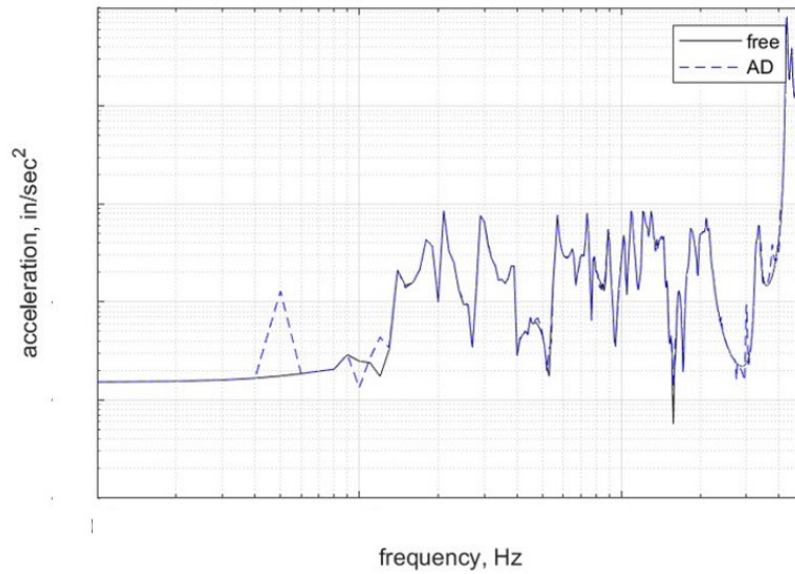


Figure 20. Booster Aft Skirt VSP1 Acceleration Y

From Figures 17 through 20, there is a minor impact to the mass-line from the frequency shift; however, it can easily be discerned and removed from data. Otherwise, AD remained computationally robust under ML frequency variations of $\pm 5\%$. There was some impact, which seemed to be constrained mostly to the “valleys” of the FRFs. Again, this should mitigate curve fitting concerns.

Field conditions include noise in the measurement channels. To respond to such reality, a noise tolerance evaluation was necessary. Two independent methodologies were developed to introduce noise into acceleration matrices and compared for verification. The recommended noise acceleration value expected during the IMT is $300 \mu\text{G rms}$. Stress test runs for the $300 \mu\text{G rms}$ case and for a $900 \mu\text{G rms}$ noise case were performed. The targeted acceleration noise levels [g] were transformed into noise acceleration [g/lb.] using a reference 2000-lb peak input force assumption. The noise was assumed correlated as it is the worst-case scenario (e.g., additive to the contaminated accelerances). Figures 21 shows the $300 \mu\text{G rms}$ random noise input signals used for this work, respectively.

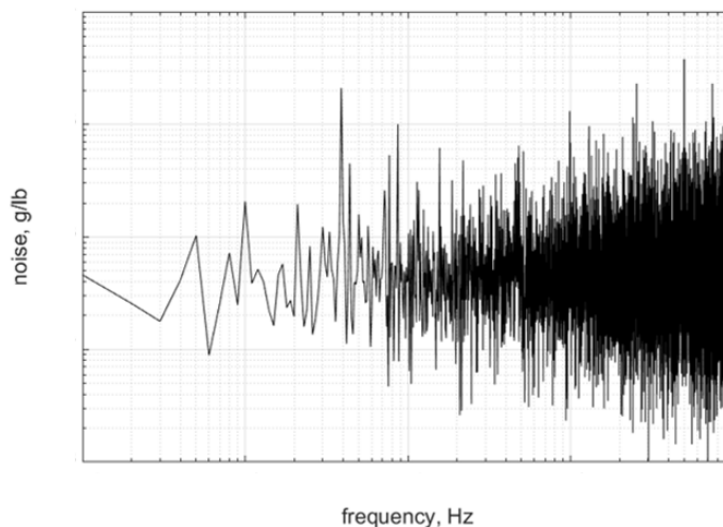


Figure 21. $300 \mu\text{G rms}$ Noise

Figures 22 and 23 provide some of the most visible impacts of the noise input to the AD process. These figures show there are some impacts, but mostly constrained to the FRF “valleys,” which should mitigate curve fitting concerns. Overall, the AD procedure remained robust under the noise introduction operations.

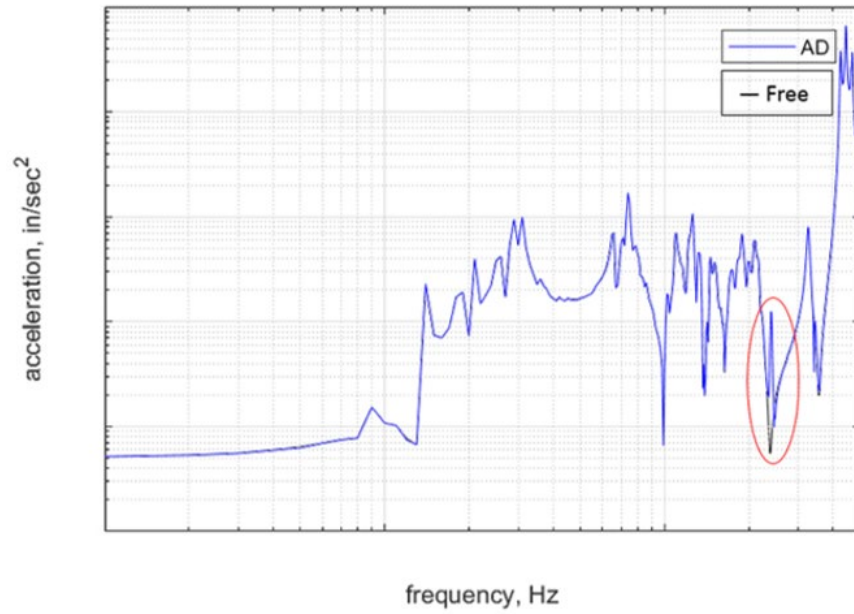


Figure 22. Booster Aft Skirt VSP1 Acceleration Z (300 μ G rms Case)

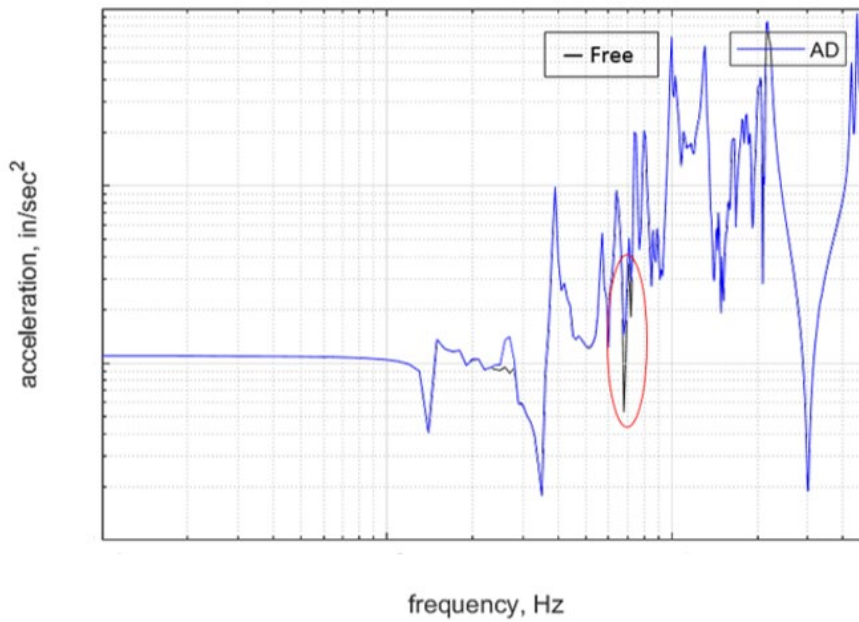


Figure 23. CS Engine Section Node

CONCLUDING REMARKS

An acceleration decoupling (AD) method has been formulated for the purpose of “subtracting out” the influence of the ML from the IMT results. With AD, the SLS decoupled FRFs are directly extracted from the IMT FRFs. The subject approach is aimed to utilize measured data only and achieve a robust FRF decoupling scheme. AD is derived from a widely used coupling technique called “Receptance Coupling”. The AD core equation reverses the RC process and utilizes a pair of auxiliary equations that enable the core equation to be resolved based on measured data only. In AD, the decoupled component FRFs are extracted from the coupled system FRFs with a transformation to remove the contribution of the “subtractive component”. The transformation is composed of a driving point acceleration at interfacing DoF and two transfer accelerances that relate interface, internal and applied force DoFs. To resolve as a function of measured data only, AD takes advantage of either testing the stand-alone ML and/or measuring the forces at the interfacing DoFs.

The work performed to date shows that the SLS free acceleration response versus coupled to ML show measurable differences which AD must overcome to be a viable procedure. To determine AD’s viability, AD numerical verification and robustness tests involved FEMs of the same integrated system configuration for the IMT. Analytical results show that AD remained computationally robust under the ML/booster interface rotational DoF stiction problem. AD remained computationally robust under ML acceleration perturbations involving damping and frequency variations on the subtractive component while the coupled system remains unchanged. Further, AD remained computationally robust under the introduction of 300 and 900 μG rms noise levels. It was also found that in the low frequency range (0.1 to 1 Hz), the unloaded ML VSP acceleration is proportional to the VSP static flexibilities. The unloaded VSP static flexibilities are a better known/less uncertain quantity, which precede the ML dynamics (modal content). This is relevant to the extraction of the SLS first free-free bending modal frequencies from the IMT (a program objective) since the AD procedure will likely require only the unloaded VSP static flexibilities to achieve this objective combination of test and model derived data.

Future work will use actual test data to exercise the AD process and provide results that can be compared back to simulations.

REFERENCES

- [1] Napolitano, K., and N. Yoder. “Fixed Base FRF Using Boundary Measurements as References – Analytical Derivation,” Proceedings of the 30th International Modal Analysis Conference, 2012.
- [2] Napolitano, K. L., Winkel, J. P., Akers, J. C., Suarez, V. J., and Staab, L. D., “Modal Survey of the MPCV Orion European Service Module Structural Test Article Using a Multi-Axis Shake Table,” Proceedings of the 36th International Modal Analysis Conference, 2018.
- [3] Allen, M. S., and Mayes, R. L., “Recent Advances to Estimation of Fixed-Interface Modal Models using Dynamic Substructuring,” Proceedings of the 36th International Modal Analysis Conference, 2018.
- [4] Neubert, Vernon H.: “Mechanical Impedance: Modelling/Analysis of Structures,” Jostens Printing and Publishing Company, Science Park Road, State College, PA 1680.1, 1987.
- [5] Cuppens, K., Sas, P., and Hermans, L., “Evaluation of the FRF Based Substructuring and Modal Synthesis Technique Applied to Vehicle FE Data,” Proceedings of the Twenty-Fifth International Seminar on Modal Analysis, Leuven Belgium, September 2000.
- [6] Allen, M.; and Mayes, R.: “Comparison of FRF and Modal Methods for Combining Experimental and Analytical Substructures,” *IMAC 2007*.
- [7] Carne, T.; and Dohrmann, C.: “Improving Experimental Frequency Response Function Matrices for Admittance Modeling,” *IMAC 2006*.
- [8] de Klerk, D.; Rixen, D.; and Voormeeren, S. N.: “General Framework for Dynamic Substructuring: History, Review, and Classification of Techniques,” *AIAA J*, Vol. 46, No. 5, May 2008.
- [9] de Klerk, D.; and Voormeeren, S. N.: “Uncertainty Propagation in Experimental Dynamic Substructuring,” *IMAC 2008*.
- [10] Ind, P.: “The Non-Intrusive Modal Testing of Delicate and Critical Structures,” Doctorate Thesis, University of London Imperial College, 2004.

- [11] Mayes et al, "Lightly Damped Experimental Substructures for Combining with Analytical Substructures," *IMAC 2007*.
- [12] Nelson C.; and Carne, T.: *Removing Undesired Periodic Data from Random Vibration Data*, Sandia Labs, 2006.
- [13] Nelson C.; and Dohrmann C.: *Using Modal Test to Estimate Support Properties*.
- [14] Sjoval, P.; and Abrahamsson, T.: Substructure system identification from coupled system data, *Mechanical and Signal Processing*, 22 (2008) 15-33.
- [15] Majed, A., Henkel, E., and Wilson, C., "Improved Method of Mixed-Boundary Component-Mode Representation for Structural Dynamic Analysis", *Journal of Spacecraft and Rockets*, Vol. 42, No. 5, Sept-Oct 2005.
- [16] Sills, J.; Majed, A.; Henkel, E.: A Deformed Geometry Synthesis Technique for Determining Stacking and Cryogenically Induced Preloads for the Space Launch System. *IMAC 38*, February 10-13, 2020, Houston, TX.